4-15-2007

Global properties of fp-shell interactions in many-nucleon systems

K. D. Sviratcheva
Louisiana State University

J. P. Draayer
Louisiana State University

J. P. Vary
Iowa State University

Recommended Citation

Sviratcheva, K., Draayer, J., & Vary, J. (2007). Global properties of fp-shell interactions in many-nucleon systems. *Nuclear Physics A, 786* (1-4), 31-46. https://doi.org/10.1016/j.nuclphysa.2007.01.087

UCRL-JRNL-222549

SLAC-PUB-11903

Global Properties of fp-Shell Interactions in Many-nucleon Systems

K. D. Sviratcheva[a, 1], J. P. Draayer[a], and J. P. Vary[b]

[a] *Department of Physics and Astronomy, Louisiana State University, Baton Rouge, Louisiana 70803, USA*
[b] *Department of Physics and Astronomy, Iowa State University, Ames, IA 50011, USA*
Lawrence Livermore National Laboratory, Livermore, California 94551
Stanford Linear Accelerator Center, Stanford University, Stanford, California 94309

Abstract

Spectral distribution theory, which can be used to compare microscopic interactions over a broad range of nuclei, is applied in an analysis of two modern effective interactions based on the realistic CD-Bonn potential for $0\hbar\Omega$ no-core shell model calculations in the fp shell, as well as in a comparison of these with the realistic shell-model GXPF1 interaction. In particular, we explore the ability of these interaction to account for the development of isovector pairing correlations and collective rotational motion in the fp shell. Our findings expose the similarities of these two-body interactions, especially as this relates to their pairing and rotational characteristics. Further, the GXPF1 interaction is used to determine the strength parameter of a quadrupole term that can be used to augment an isovector-pairing model interaction with Sp(4) dynamical symmetry, which in turn is shown to yield reasonable agreement with the low-lying energy spectra of ^{58}Ni and ^{58}Cu.

Key words: comparison of interactions, isovector pairing, quadrupole features, effective interactions, realistic potentials, spectral distribution theory, Sp(4) dynamical symmetry
PACS: 21.60.Fw, 21.30.Fe, 21.10.Re, 21.60.Cs

[1] Corresponding author.
E-mail address: kristina@baton.phys.lsu.edu;
Phone: +225-578-0351; *Fax:* +225-578-5855

1 Introduction

Realistic NN potentials, whether derived from meson exchange theory (e.g.,[1]) or chiral effective field theory (e.g.,[2]), and their effective interaction derivatives, provide no *a priori* indication regarding how well they may or may not reproduce prominent features of nuclei, such as pairing gaps in nuclear energy spectra or enhanced electric quadrupole transitions in collective rotational bands, until actually employed in shell-model calculations. While such calculations are often laborious and model dependent, a simple and straightforward evaluation of an interaction can be made using spectral distribution theory [3,4]. Indeed, spectral distribution methods can yield a deeper understanding of the nature of an interaction and above all, its role in the development of collective and correlated many-nucleon motion [5,6,7,8,9,10,11,12]. In particular, spectral distribution theory can be used to show through correlation coefficient measures the similarity of interactions. Such analyses are independent of the averages of the interactions and yield an overall comparison across a broad domain of nuclei beyond what can be achieved by overlaps of nuclear states or detailed comparisons of two-body interaction matrix elements.

In this paper we examine three modern fp-shell interactions, specifically, two interactions denoted as "CD-Bonn" and CD-Bonn+3terms [13] based on the CD-Bonn realistic potential [1] as well as GXPF1 [14]. The GXPF1 effective interaction is obtained from a realistic G-matrix interaction based on the Bonn-C potential [15] by adding empirical corrections determined through systematic fitting to experimental energy data in the fp shell. The CD-Bonn potential is a charge-dependent one-boson-exchange nucleon-nucleon (NN) interaction that is one of the most accurate in reproducing the available proton-proton and neutron-proton scattering data. Specifically, we use two-body matrix elements of an effective "CD-Bonn" interaction derived from the CD-Bonn potential for $0\hbar\Omega$ no-core shell model (NCSM) calculations in the fp shell. In addition, the CD-Bonn+3terms interaction introduces phenomenological isospin-dependent central terms plus a tensor force with strengths and ranges determined in $0\hbar\Omega$ NCSM calculations to achieve an improved description of the $A = 48$ Ca, Sc and Ti isobars. In the regard, we use spectral distribution theory to provide an assessment of differences between the novel CD-Bonn+3terms interaction and "CD-Bonn"as well as a comparison of these interactions with GXPF1, which has been shown to reproduce nuclear energy spectra throughout the fp shell [14].

The likely success of the three interactions for reproducing pairing and rotational spectral features is examined in a comparison to a pairing-plus-quadrupole model interaction, which combines a Sp(4) dynamically symmetric model interaction [16,17] for description of like-particle and proton-neutron (isovector) pairing correlations with a SU(3) symmetric term that governs a shape-

determined dynamics. If the model and effective interactions are strongly correlated, then the latter will reflect the characteristic properties of the simpler model Hamiltonian, which in turn may be used as a good approximation.

The present study, which is complementary to a similar $1f_{7/2}$ analysis [18], focuses on the upper *fp*-shell domain, which includes neutron-deficient and $N \approx Z$ nuclei along the nucleosynthesis *rp*-path and unstable nuclei currently explored in radioactive beam experiments [19,20]. The analysis of the upper *fp* results reveals overall properties of the interactions under consideration different from those observed in the $1f_{7/2}$ orbit.

Several detailed reviews of the nuclear shell model and its applications have been published recently [21,22,23] that delve into related key physics issues that are explored in the present work. However, the spectral distribution analysis provided here is novel and sheds considerable light on the features of new fp-shell interactions, some of which have been developed since those reviews were completed.

2 Theoretical Framework

The theory of spectral distributions is an excellent approach for studying microscopic interactions [4,24,25] and continues to be a powerful concept with recent applications in quantum chaos, nuclear reactions and nuclear astrophysics including studies on nuclear level densities, transition strength densities, and parity/time-reversal violation (for example, see [26,27,28,29,30,31,32,33,34,35]). The significance of the method is related to the fact that low-order energy moments over a certain domain of single-particle states, such as the energy centroid of an interaction (its average expectation value) and the deviation from that average, yield valuable information about the interaction that is of fundamental importance [7,11,25,36,37,38,39,40,41] without the need for carrying out large-dimensional matrix diagonalization and with little to no limitations due to the dimensionality of the vector space. Note that if one were to include higher-order energy moments, one would obtain more detailed results that, in principle, should eventually reproduce those of conventional microscopic calculations.

Spectral distribution theory (see Appendix for basic mathematical definitions and notation introduction) combines important features, the most significant of which are as follows:

(1) The theory provides a precise measure, namely, the correlation coefficient, for the overall similarity of two interactions. Literally the correlation coefficient is a measure of the extent to which two interactions "look like"

(are correlated with) one another. In this respect, correlation coefficients can be used to extract information how well pairing/rotational features are developed in interactions, which may differ substantially from an individual comparison of pairing/quadrupole interaction strengths [18].

(2) It gives an exact prescription for identifying the *pure* zero- (centroid), one- and two-body parts of an interaction under a given space partitioning. Therefore, major properties follow:
   (a) The correlation coefficients are independent of the interaction centroids. (A direct comparison of two-body matrix elements provided by NN potentials may be misleading, especially when the averages of the interactions differ considerably.)
   (b) The pure one-body part of an interaction, the so-called induced single-particle energies (Eq. 14), is naturally identified in the framework of spectral distribution theory and is indeed the average monopole interaction (compare to [14]). As such it influences the evolution of the shell structure, shell gaps and binding energies [42].
   (c) The pure two-body part is essential for studies of detailed property-defining two-body interactions beyond strong mean-field effects.

(3) The correlation coefficient concept can be propagated straightforwardly beyond the defining two-nucleon system to derivative systems with larger numbers of nucleons [4] and higher values of isospin [6]. This, in addition to the two-nucleon information provided by alternative approaches (e.g.,[43]), yields valuable overall information, without a need for carrying out extensive shell-model calculations, about the universal properties of a two-body interaction in shaping many-particle nuclear systems.

Group theory underpins spectral distribution theory [3,4,6,8,44]. The model space is partitioned according to particular group symmetries and each subsequent subgroup partitioning yields finer and more detailed spectral estimates. Specifically, for n particles distributed over 4Ω single-particle states, the spectral distribution averaged over all n-particle states associated with the $\mathrm{U}(4\Omega)$ group structure is called a *scalar* distribution (denoted by "n" in the formulae) and the spectral distribution averaged over the ensemble of all n-particle states of isospin T associated with $\mathrm{U}(2\Omega) \otimes \mathrm{U}(2)_T$ is called an *isospin-scalar* distribution (denoted by "n, T").

For a spectral distribution α (α is n or n, T), the correlation coefficient between two Hamiltonian operators, H and H', is defined as

$$\zeta^{\alpha}_{H,H'} = \frac{\langle (H^{\dagger} - \langle H^{\dagger} \rangle^{\alpha})(H' - \langle H' \rangle^{\alpha}) \rangle^{\alpha}}{\sigma_H \sigma_{H'}} = \frac{\langle H^{\dagger} H' \rangle^{\alpha} - \langle H^{\dagger} \rangle^{\alpha} \langle H' \rangle^{\alpha}}{\sigma_H \sigma_{H'}}, \quad (1)$$

where the "width" of H is the positive square root of the variance,

$$(\sigma^{\alpha}_H)^2 = \langle (H - \langle H \rangle^{\alpha})^2 \rangle^{\alpha} = \langle H^2 \rangle^{\alpha} - (\langle H \rangle^{\alpha})^2, \quad (2)$$

and the steps for computing these quantities are outlined in the Appendix. The average values, $\langle\hat{O}\rangle^{\alpha}$, related to the trace of an operator $\hat{O}$ divided by the dimensionality of the space, are given in terms of the ensemble considered. In the (isospin-)scalar case, the correlation will be denoted by ζ^{n} ($\zeta^{n,T}$) or simply ζ (ζ^{T}) for $n = 2$. The significance of a positive correlation coefficient is given by Cohen [45] and later revised to the following table:

Table 1
Interpretation of a correlation coefficient.

trivial	small	medium	large	very large	nearly perfect	perfect
0.00-0.09	0.10-0.29	0.30-0.49	0.50-0.69	0.70-0.89	0.90-0.99	1.00

From a geometrical perspective, in spectral distribution theory every interaction is associated with a vector and the correlation coefficient ζ (Eq. 1) defines the angle (via a normalized scalar product) between two vectors of length σ (Eq. 2). Hence, $\zeta_{H,H'}$ gives the normalized projection of H onto the H' interaction (or H' onto H). In addition, $(\zeta_{H,H'})^2$ gives the percentage of H that reflects the characteristic properties of the H' interaction.

The pairing and rotational characteristics of an interaction can be probed through its projection onto a model microscopic Hamiltonian that describes isovector pairing correlations and collective rotational excitations. While the latter possess a clear SU(3) symmetry [49] within the framework of the harmonic oscillator shell model, the former respect a Sp(4) dynamical symmetry [46,47,48]. Specifically, we employ the pairing-plus-quadrupole model interaction

$$H_M = H_{\mathfrak{sp}(4)} + H_Q^{\perp}(2),\ H_Q = -\frac{\chi}{2} Q\cdot Q, \tag{3}$$

where $H_{\mathfrak{sp}(4)}$ is an isoscalar Sp(4)-dynamically symmetric interaction [17] for a system of n valence nucleons (an eigenvalue of $\hat{N}$) in a 4Ω-dimensional space,

$$H_{\mathfrak{sp}(4)} = -G\sum_{i=-1}^{1}\hat{A}_i^{\dagger}\hat{A}_i - \tfrac{E}{2\Omega}(\hat{T}^2 - \tfrac{3\hat{N}}{4}) - C\tfrac{\hat{N}(\hat{N}-1)}{2} - \epsilon\hat{N}, \tag{4}$$

with two-body antisymmetric JT-coupled matrix elements (Appendix Eq. 6) for $\{r \leq (s,t);\ t \leq u\}$ orbits,

$$W^{JT}_{rstu} = -G_0\tfrac{\sqrt{\Omega_r\Omega_t}}{\Omega}\delta_{J0}\delta_{T1}\delta_{rs}\delta_{tu} - \{-E_0[(-)^T + \tfrac{1}{2}] + C\}\delta_{rt}\delta_{su}, \tag{5}$$

where $G_0 = G + \frac{F}{3},\ E_0 = (\frac{E}{2\Omega} + \frac{D}{3})$, G, F, E, D and C are interaction strength parameters and $\epsilon > 0$ is the Fermi level energy (see Table I in Ref.[17] for parameter estimates). The $\mathfrak{sp}(4)$ algebraic structure is exactly the one needed in nuclear isobaric analog 0^+ states to describe proton-proton (pp), neutron-neutron (nn) and proton-neutron (pn) isovector pairing correlations (accounted by the pair annihilation (creation) operators $\hat{A}^{(\dagger)}_{+1,-1,0}$) and isospin

symmetry. The latter is reflected by the isospin operator $\hat{T}^2$ and related to a J-independent isoscalar ($T = 0$) pn force. The most general model interaction with Sp(4) dynamical symmetry [17] has been found to provide for a reasonable microscopic description of the pairing-governed isobaric analog 0^+ states in light and medium mass nuclei and to account quite well for the observed detailed structure beyond mean-field effects such as the $N = Z$ anomalies, isovector pairing gaps and staggering effects [16]. In addition, the $H_{\mathfrak{sp}(4)}$ interaction (4) has been shown to strongly correlate, especially when the quadrupole term is introduced, with the "CD-Bonn", CD-Bonn+3terms and GXPF1 interactions in the $1f_{7/2}$ orbit [18].

The $H_Q^{\perp}(2)$-term in (Eq. 3) is the part of the pure two-body $H_Q(2)$ quadrupole-quadrupole interaction that, in the vector algebra terminology, is orthogonal to the pure two-body Sp(4) Hamiltonian [7]. This is because the Sp(4) interaction contains a part of the quadrupole-quadrupole interaction that is not negligible as revealed by the correlation between H_Q and $H_{\mathfrak{sp}(4)}$. Namely, in the scalar case it is 15% ($1f_{7/2}$), 29% ($1f_{5/2}$) and 29% ($2p_{1/2}2p_{3/2}$), and for the T=1 part of the interactions, it is 34% ($1f_{7/2}$), 58% ($1f_{5/2}$) and 58% ($2p_{1/2}2p_{3/2}$).

Such a Hamiltonian (Eq. 3) does not affect the centroid of $H_{\mathfrak{sp}(4)}$ because $H_Q^{\perp}(2)$ is traceless. In this way this collective interaction preserves the shell structure that is built into $H_{\mathfrak{sp}(4)}$ and established by a harmonic oscillator potential and as a result is favored in many studies [7,11].

3 Results and Discussions

The similarity of the "CD-Bonn", CD-Bonn+3terms and GXPF1 interactions, which will be denoted as H_0, and their pairing/rotational characteristics can be tracked in many-nucleon systems [10] through the propagation formulae (Appendix Eqs. 12, 16). The latter determine how the averages extracted from the two-nucleon matrix elements get carried forward into many-nucleon systems. This propagation of information is model-independent.

The present investigation focuses on the upper *fp*-shell domain and is complementary to a similar $1f_{7/2}$ analysis [18] (a few results from that study are presented in Section 3.1 for completeness). Such a partitioning of the fp oscillator shell follows naturally from a splitting of these two regions by a strong spin-orbit interaction. We examine the $H_0(2)$ pure two-body part of the fp-shell interactions and how it is correlated to the model interaction (Eq. 3). The latter, in addition to its centroid, is pure two-body in the upper *fp* model space because of the assumption for $H_{\mathfrak{sp}(4)}$ of constant Fermi level energy and fixed interaction strengths throughout the entire region. The significance of the correlation coefficients between pure two-body interactions [25] reflect the

fact that nuclear states, their collective properties and configuration mixing, are solely shaped by the pure two-body part of an interaction, while the one-body part, albeit of a considerable significance, trivially reorders the states in the nuclear energy spectrum. In addition, such analyses are free of the one-body influence including induced single-particle energies, which are related to the monopole interaction [43,42,14], and external single-particle energies. The latter are introduced when a core is assumed, as for the $0\hbar\Omega$ ^{40}Ca-core shell model using the GXPF1 interaction. For the $0\hbar\Omega$ NCSM calculations with "CD-Bonn" or CD-Bonn+3terms, the two-body matrix elements specifying the particle-core interactions supplant the role of external single-particle energies. These additional two-body matrix elements together with the external single-particle energies for GXPF1 are not included in the present analyses.

In our study, we vary only χ, the quadrupole strength parameter in (Eq. 3), to find its optimal value (which is an exact solution) by maximizing the ζ correlation coefficient [50] between the model H_M interaction and the pure two-body part $H_0(2)$ of each of the effective interactions under consideration. We do not alter the parameters of the Sp(4) model, which have already been shown in an appropriate domain of states to be valid for reproducing various quantities (such as binding energies and pairing gaps) and are in agreement with estimates available in literature [16,17].

In both scalar (Table 2) and isospin-scalar (Fig. 1) distributions, the $\zeta^{n(T)}_{H_0(2),H_M}$ correlation with the pairing+quadrupole H_M interaction is stronger for GXPF1 compared to "CD-Bonn" and CD-Bonn+3terms. Hence, other types of interactions that do not correlate with the pairing and quadrupole-quadrupole interactions (of fixed strength throughout the upper *fp* shell) comprise a relatively small part of the pure two-body GXPF1 interaction. They are weakest for the $T = n/2$ group of states (Fig. 1) for all the three interactions. In addition, the results reveal that the symplectic Sp(4) dynamical symmetry of H_M, especially when compared to both CD-Bonn interactions and in the highest-isospin ($T = n/2$) group of states, is only slightly broken by $H^{\perp}_{Q}(2)$ (Table 2, fifth row and Fig. 1). The Sp(4) symmetry breaking is related to the correlation coefficient of $H^{\perp}_{Q}(2)$ with H_M or equivalently to the ratio of their norms [51], where $(\zeta_{H_M,H^{\perp}_{Q}(2)})^2 = 1 - (\zeta_{H_M,H_{\mathfrak{sp}(4)}})^2 = 1 - R_{\mathrm{Sp(4)}}$ (Table 2).

Two correlation coefficients, which in the present study are independent of any interaction strength parameters, are of particular interest. Specifically, the isospin-scalar space partitioning is where the ability of an interaction to form correlated pairs and hence reproduce prominent pairing gaps is detected via $\zeta^{n,T}_{H_0(2),H_{\mathfrak{sp}(4)}}$. The capability of an interaction to describe rotational collective motion, and hence to reproduce rotational bands and enhanced electric quadrupole transitions, can be detected via its correlation to the full $H_Q(2)$ quadrupole-quadrupole two-body interaction, $\zeta^{n(T)}_{H_0(2),H_Q(2)}$.

The results show a large correlation with isovector pairing of the $T = 1$ part of the fp-shell interactions under considerations ($n = 2$), especially for GXPF1, and a good tendency towards development of pairing correlations in the $T = n/2$ states (Fig. 1). In both scalar and isospin-scalar cases (Table 2, fourth row and Fig. 2), the rotational features are more fully developed for GXPF1 and less for CD-Bonn+3terms and "CD-Bonn" (Fig. 2) different from the outcome in the $1f_{7/2}$ region especially for the $T = 1$ part of "CD-Bonn".

In short, the GXPF1 interaction is expected to reproduce spectral features like pairing gaps and rotational bands observed in the upper *fp* nuclei, while it is unlikely for both CD-Bonn interactions to fully reflect the rotational properties of these nuclei. In comparison, the CD-Bonn+3terms interaction in the $1f_{7/2}$ orbit exhibits well-developed pairing and rotational characteristics [18]. Such a difference in the behavior of CD-Bonn+3terms within both regions, $1f_{7/2}$ and upper *fp*, may reflect the fact that this interaction was determined through a reproduction of the low-lying energy spectrum and binding energy of $A = 48$ $1f_{7/2}$ nuclei.

The different extent to which the GXPF1 interaction compared to the "CD-Bonn" and CD-Bonn+3terms interactions reflects development of pairing correlations and collective rotational modes in the upper *fp* domain may be the reason why their pure two-body part do not correlate strongly as, for example, "CD-Bonn" and CD-Bonn+3terms do. Namely, in the (isospin-) scalar case the pure two-body correlations [2] are 0.90 (0.88) between "CD-Bonn" and CD-Bonn+3terms and only 0.56 (0.37) between "CD-Bonn" and GXPF1 and 0.53 (0.40) between CD-Bonn+3terms and GXPF1. In addition, the isospin-scalar correlation coefficients involving the significant induced pure one-body (monopole) contribution, λ_j^T (Appendix Eq. 14), differ between GXPF1 and the two "CD-Bonn" interactions. Their behavior, especially below mid-shell, reflects the similarity of the corresponding $T = 0$ induced single-particle energies and the opposite signs of the corresponding $\lambda^{T=1}_{2p_{3/2}}$ and $\lambda^{T=1}_{1f_{5/2}}$.

In summary, when compared to the original "CD-Bonn", $0\hbar\Omega$ NCSM calculations with CD-Bonn+3terms for upper *fp* nuclei are likely to achieve an improved description of many-body spectral phenomena, associated with pair formation (especially when $T \neq n/2$) and with rotational motion (especially in the highest-isospin states). While such results lie slightly closer to what is achieved by the GXPF1 interaction with two-body matrix elements directly adjusted to experimental fp-shell data, larger NSCM model spaces for both CD-Bonn interactions may be necessary for a better reproduction of pairing and rotational spectral features throughout the upper *fp* domain.

[2] In the isospin-scalar case, the correlations vary slightly with the particle number and isospin and average values are quoted.

3.1 Individual-Orbit Analysis

One can further perform a partitioning of the fp-space to single-j orbits, $1f_{7/2}$, $1f_{5/2}$, $2p_{1/2}$ and $2p_{3/2}$, to provide for more detailed spectral measures that may reflect important fine effects that are otherwise averaged out when the entire fp major shell is taken into account. We have already illustrated such an example and its significance by exploration of the $1f_{7/2}$ orbit [18]. Individual orbit analyses render correlation coefficients that are free of the influence of any one-body interaction [by definition, (Appendix Eq. 7,9,14)]. However, due to the small model space, the $2p_{1/2}$ and $2p_{3/2}$ orbits are combined and in their joint region only the pure two-body part of the interactions is considered.

In the scalar distribution, a good portion, 53% to 98%, of the H_M pairing+quadrupole model interaction is described solely by the $H_{\mathfrak{sp}(4)}$ interaction ($R_{\mathrm{Sp}(4)}$, Table 3). The H_0 fp-shell interactions exhibit a quite well-developed rotational character (Table 3, ζ_{H_0,H_Q}) except for "CD-Bonn" and CD-Bonn+3terms in the $2p_{1/2}2p_{3/2}$ region. Besides these cases, the H_M model interaction, as revealed by ζ_{H_0,H_M} in Table 3, can be used as a very good approximation to the fp-shell interactions within each of the domains considered.

The $\zeta^{T=1}_{H_0,H_{\mathfrak{sp}(4)}}$ correlation coefficients (Table 4) show large $J = 0$ isovector coherence within each single-j shell, particularly for the $T = 1$ part of CD-Bonn+3terms and GXPF1, which are expected to describe quite well phenomena of a pairing character, while for "CD-Bonn" other types of interaction compete with pair formation. The latter are of the $H^{\perp}_{Q}(2)$ type for the $1f_{7/2}$ and $1f_{5/2}$ orbits, where the residual interactions are negligible. In short, the simple Sp(4) model interaction and especially its extended pairing+quadrupole H_M interaction can reproduce reasonably well the $T = 1$ part of the three effective interactions under consideration within the orbits specified in Table 4.

Within individual orbits a very close similarity is observed between the effective and model interactions as well as in nuclear systems with more than two nucleons. However, more prominent differences among the interactions appear in the multi-j upper fp domain especially concerning both "CD-Bonn" interactions. This may indicate that the inter-orbit interactions do not respect strongly the symmetries imposed in the model interaction. In addition, the interaction strengths may differ from one orbit to another. While they do not affect correlation coefficients in the singe-j cases, their relative strength is of a great importance for multi-j analysis.

3.2 Energy Spectra for $A = 58$ Nuclei

The results presented above show that the H_M model Hamiltonian (Eq. 3) can be used in the upper *fp* region as a quite good approximation of the pure two-body part of the GXPF1 interaction (Table 2 and Fig. 1). This implies that both interactions are expected to yield energy spectra of a similar pattern.

As an illustrative example, we apply the simpler model interaction (Eq. 3) to a nuclear system of two nucleons in the upper *fp* region without any parameter variation. Particularly, we assume a ^{56}Ni-core and that both nucleons in ^{58}Ni and ^{58}Cu occupy the upper *fp* orbits with reasonable probability [14]. For a description of the low-lying structure of these nuclei, external single-particle energies are needed to rescale at the end the eigenvalues of the model Hamiltonian. This is performed trivially due to the microscopic structure of the model eigenstates, which are constructed in terms of fermion creation operators. We adopt single-particle energies that are derived from the ^{57}Ni energy spectrum. To a very reasonable degree, these energies reflect the influence of the $1f_{7/2}$ orbit and the core mean-field contribution.

The model Hamiltonian uses a χ value of 0.027 that we obtained through a comparison of H_M to GXPF1 within a scalar distribution. The reason is that the pure two-body GXPF1 interaction holds the best correlation coefficient to the model interaction in the upper *fp* region (Table 2). In addition, the energy spectra for ^{58}Ni and ^{58}Cu are found to be closely reproduced by shell model calculations with the GXPF1 interaction in the full fp shell [14].

We extend the model space to include the $1g_{9/2}$ orbit as it intrudes in the upper *fp* domain. This is exactly the space where the Sp(4) model was applied and interaction strength parameters determined [17]. The results (Fig. 3) show a very good reproduction of the low-lying $T = 1$ spectra in ^{58}Ni and ^{58}Cu, especially the lowest 2^+ states for both nuclei and the first 0^+ ($T = 1$) state above the ^{58}Cu ground state. Both states are of particular significance. On the one hand, the energy difference between the lowest 0^+ and 2^+ states is believed to be directly affected by the formation of correlated pairs in the lowest 0^+ state (ground state for even-even nuclei) and the pairing gap that occurs below the first excited 2^+ state of a broken pair. On the other hand, the $0^+(T = 1)$ to $1^+(T = 0)$ energy difference in $N = Z$ odd-odd nuclei is associated with the close interplay of isovector (T=1, pairing correlations) and isoscalar (T=0) interactions between protons and neutrons in the same major shell. In addition, the $T = 0$ spectrum of ^{58}Cu as predicted by the model interaction possesses the same pattern of the levels observed, namely, the 1^+ ground state is followed by 3^+, 1^+, 2^+, 4^+, and 3^+. The ^{58}Cu $T = 0$ spectrum appears narrower than the experimental data, which suggests that different quadrupole strengths for $T = 0$ and $T = 1$ need to be used.

In short, we demonstrate that strong correlations typically yield very similar energy spectra and reproduction of the overall pattern of the energy levels without any adjustment of the interaction strength parameters.

4 Conclusions

In the present article, we have compared three modern fp-shell interactions, "CD-Bonn", CD-Bonn+3terms, and GXPF1, based on realistic nucleon-nucleon potentials, in the upper fp region by means of the theory of spectral distributions. We focused on the weaker but property-defining two-body part of the interactions and studied their pairing and rotational character in a comparison to a pairing+quadrupole model interaction, which includes Sp(4) dynamically symmetric isovector pairing correlations and a proton-neutron isoscalar force together with a quadrupole-quadrupole interaction for description of SU(3) dynamically symmetric collective rotational mode.

The outcomes show that the pure two-body GXPF1 interaction, which is adjusted through systematic fitting to experimental energy data in the fp shell, demonstrates well developed collective rotational features and a tendency of its $T = 1$ part towards formation of correlated pairs. In addition, it strongly correlates with the pairing+quadrupole H_M model interaction, which is reflected in the quite good agreement between the experimental low-lying energy spectra of ^{58}Ni and ^{58}Cu and the theoretical prediction based on H_M in the $1f_{5/2}2p_{1/2}2p_{3/2}1g_{9/2}$ major shell. Individual-orbit analysis, including the $1f_{7/2}$, $1f_{5/2}$, $2p_{1/2}$, and $2p_{3/2}$ levels, shows considerably stronger correlation to H_M (up to $0.8 - 1.00$) and a clear pairing or/and rotational character for all the three fp-shell interactions, which in addition correlate more strongly among themselves. In this respect, inter-orbit interactions may be a reason why both CD-Bonn interactions suitable for $0\hbar\Omega$ NCSM fp-shell calculations invoke small to medium pure two-body correlations in the upper fp domain. While these correlations for CD-Bonn+3terms appear slightly superior to the ones for "CD-Bonn"due to a phenomenological correction, it may be interesting to investigate how they vary for effective interactions based on the realistic CD-Bonn potential when higher-$\hbar\Omega$ configurations are included in the no-core shell model analysis.

In summary, based on these results, spectral distribution theory appears to be a good framework for uncovering fundamental properties of realistic interactions and their effective interaction derivatives in many-nucleon systems. We find varying degrees of respect for selected underlying symmetries. As some of these symmetries have been demonstrated to be important for certain spectral features, we have a tool for rapidly assessing the likely success of these interactions for reproducing those spectral features. For example, it is unlikely that

the CD-Bonn+3terms interaction will provide a fully satisfactory description of the rotational properties of nuclei in the upper *fp* shell. Given that this interaction was determined only with $A = 48$ nuclear spectra and binding energies [13], future efforts at expanding the region of its validity in the no-core shell model should benefit from the analysis provided here.

Acknowledgments

One of us (JV) would like to thank Sorina Popescu, Sabin Stoica and Geanina Negoita for valuable discussions. This work was supported by the US National Science Foundation, Grant Numbers 0140300 & 0500291, and the Southeastern Universities Research Association. This work was partly performed under the auspices of the US Department of Energy by the University of California, Lawrence Livermore National Laboratory under contract No. W-7405-Eng-48 and under the auspices of grants DE-FG02-87ER40371 & DE–AC02–76SF00515.

Appendix

The theory of spectral distributions (or statistical spectroscopy) is well documented in the literature [3,4,37,6,8] and is accompanied by computational codes [8,52] for evaluating various measures. The purpose of this appendix is to specify the notation and ensure that our definitions of the summations and numerical factors that enter into such measures are clearly understood.

In standard second quantized form, a one- and two-body interaction Hamiltonian is given in terms of fermion creation $a^\dagger_{jm(1/2)\sigma} = c^\dagger_{jm(1/2)\sigma}$ and annihilation $a_{j-m(1/2)-\sigma} = (-1)^{j-m+1/2-\sigma} c_{jm(1/2)\sigma}$ tensors, which create or annihilate a particle of type $\sigma = \pm 1/2$ (proton/neutron) in a state of total angular momentum j (half integer) with projection m in a finite space $2\Omega = \Sigma_j(2j+1)$,

$$H = -\sum_{r\le s} \sqrt{[r]}\varepsilon_{rs}\{a^\dagger_r \otimes a_s\}^{(00)} \\ -\frac{1}{4}\sum_{rstu\Gamma} \sqrt{(1+\delta_{rs})(1+\delta_{tu})[\Gamma]} W^\Gamma_{rstu}\{\{a^\dagger_r \otimes a^\dagger_s\}^\Gamma \otimes \{a_t \otimes a_u\}^\Gamma\}^{(00)}, \quad (6)$$

where the labels are $r = \{j_r, \tau_r = \frac{1}{2}\}$, $[r] = 2(2j_r+1)$, and $[\Gamma] = (2J+1)(2T+1)$. In (Eq. 6), ε_{rs} is the (external) single-particle energy (hereafter we consider no angular momentum degeneracy for two different radial quantum numbers, $\varepsilon_{rs} = \varepsilon_r\delta_{rs}$) and $W^{JT}_{rstu} = < rsJTMT_0|H|tuJTMT_0 >$ is the two-body antisymmetric matrix element in the JT-coupled scheme [$W^\Gamma_{rstu} = -(-)^{r+s-\Gamma}W^\Gamma_{srtu} = -(-)^{t+u-\Gamma}W^\Gamma_{rsut} = (-)^{r+s-t-u}W^\Gamma_{srut} = W^\Gamma_{turs}$]. For an isospin nonconserving two-body interaction of isospin rank $\mathcal{T}$, the coupling of fermion operators is

as follows, $\{\{a_r^\dagger \otimes a_s^\dagger\}^{JT} \otimes \{a_t \otimes a_u\}^{JT}\}^{(0\mathcal{T})}$, with $W_{rstu}^{(\mathcal{T})JT}$ matrix elements.

For a major shell that consists of several s orbits, each of degeneracy $\mathcal{N}_s$ ($\mathcal{N} = \sum_s \mathcal{N}_s$), the (traceless) external single-particle energy of the $r^{\rm th}$ orbit is obtained as

$$\tilde{\varepsilon}_r = \varepsilon_r - \varepsilon = \varepsilon_r - \frac{1}{\mathcal{N}} \sum_s \varepsilon_s \mathcal{N}_s, \tag{7}$$

where the average (external) single-particle energy is $\varepsilon = \frac{1}{\mathcal{N}} \sum_s \varepsilon_s \mathcal{N}_s$.

Scalar Distribution. For a two-particle system, the monopole moment (centroid), which is the average expectation value of the two-body interaction, is defined in the scalar case as

$$W_c = \frac{1}{\binom{\mathcal{N}}{2}} \sum_{r \le s, \Gamma} [\Gamma] W_{rsrs}^{\Gamma} = \frac{\sum_{rs,\Gamma} [\Gamma] W_{rsrs}^{\Gamma} (1+\delta_{rs})}{\mathcal{N}(\mathcal{N}-1)}, \tag{8}$$

where $\mathcal{N} = 4\Omega = 2\sum_r (2j_r+1)$, the Γ-sum goes over all possible (J,T) for given r,s, and $\binom{\mathcal{N}}{2} = \sum_{r \le s,\Gamma} [\Gamma]$. The traceless induced single-particle energy is constructed by contraction of the two-body interaction into an effective one-body operator under the particular group structure,

$$\lambda_r = \frac{1}{\mathcal{N}_r} \sum_{s,JT} [JT] W_{rsrs}^{JT} (1+\delta_{rs}) - \frac{1}{\mathcal{N}} \sum_{tu,JT} [JT] W_{tutu}^{JT} (1+\delta_{tu}). \tag{9}$$

For a system with one hole in the $r^{\rm th}$ orbit, λ_r corresponds to the energy of a single particle as contributed by the interaction with the valence particles above the core. In turn, the traceless pure two-body interaction is defined as

$$W_{rstu}^{JT}(2) = W_{rstu}^{JT} - (W_c + \frac{\lambda_r + \lambda_s}{\mathcal{N}-2}) \delta_{rt} \delta_{su}. \tag{10}$$

In order to calculate energy moments and their propagation for higher n (and T) values, each interaction H (consisting of one($k=1$)- and two($k=2$)-body parts) needs to be expressed as a linear combination of terms of definite particle rank (irreducible tensors $\mathcal{H}_k(\nu)$ of rank $\nu = 0,1,2$), that is as a collection of pure zero-, one- and two-body interactions. For n particles, the Hamiltonian can be rendered (the sum $\sum^*$ goes over $r \le s$, $t \le u$ and $\Gamma = (J,T)$),

$$\begin{aligned} H =& n\mathcal{H}_1(0) + \binom{n}{2} \mathcal{H}_2(0) + \mathcal{H}_1(1) + (n-1)\mathcal{H}_2(1) + \mathcal{H}_2(2) \\ =& -n\varepsilon - \binom{n}{2} W_c - \sum_r [r]^{\frac{1}{2}} (\tilde{\varepsilon}_r + \frac{n-1}{\mathcal{N}-2} \lambda_r) \{a_r^\dagger \otimes a_r\}^{(00)} \\ & - \sum\nolimits^* \frac{\sqrt{[\Gamma]}}{\sqrt{(1+\delta_{rs})(1+\delta_{tu})}} W_{rstu}^{\Gamma}(2) \{\{a_r^\dagger \otimes a_s^\dagger\}^{\Gamma} \otimes \{a_t \otimes a_u\}^{\Gamma}\}^{(00)}, \end{aligned} \tag{11}$$

for then the quantity that defines the correlation coefficient (Eq. 1) is easily computed for different particle numbers n,

$$\langle H^\dagger H'\rangle^n - \langle H^\dagger\rangle^n\langle H'\rangle^n = \frac{n(\mathcal{N}-n)}{\mathcal{N}(\mathcal{N}-1)}\sum_r[\tilde{\varepsilon}_r + \frac{n-1}{\mathcal{N}-2}\lambda_r][\tilde{\varepsilon}'_r + \frac{n-1}{\mathcal{N}-2}\lambda'_r]\mathcal{N}_r$$
$$+\frac{n(n-1)(\mathcal{N}-n)(\mathcal{N}-n-1)}{\mathcal{N}(\mathcal{N}-1)(\mathcal{N}-2)(\mathcal{N}-3)}\sum{}^*[\Gamma]W^\Gamma_{rstu}(2)W'^\Gamma_{rstu}(2). \qquad (12)$$

Isospin-Scalar Distribution. Analogously, the centroid is defined as,

$$W_c^T = \frac{2}{\mathcal{N}(\mathcal{N}+(-1)^T)}\sum_{r\le s,J}[J]W^{JT}_{rsrs} \qquad (13)$$

where $\mathcal{N}=2\Omega$. The λ_r^T traceless induced single-particle energy for orbit r and the $W^{JT}_{rstu}(2)$ traceless pure two-body interaction [8] are defined as,

$$\lambda_r^T = \frac{1}{\mathcal{N}_r}\sum_{s,J}[J]W^{JT}_{rsrs}(1+\delta_{rs}) - \frac{1}{\mathcal{N}}\sum_{tu,J}[J]W^{JT}_{tutu}(1+\delta_{tu}), \qquad (14)$$

$$W^{JT}_{rstu}(2) = W^{JT}_{rstu} - (W_c^T + \frac{\lambda_r^T+\lambda_s^T}{\mathcal{N}+2(-1)^T})\delta_{rt}\delta_{su}. \qquad (15)$$

In order to calculate the correlation coefficient $\zeta^{n,T}$ and the variance $\sigma^{n,T}$, the following quantities are needed (the sum $\sum^*$ goes over $r\le s$, $t\le u$ and J),

$$\langle H^\dagger H'\rangle^{n,T} - \langle H^\dagger\rangle^{n,T}\langle H'\rangle^{n,T} = p_1(T)\sum_r\mathcal{N}_r\tilde{\varepsilon}_r\tilde{\varepsilon}'_r + \sum_{r,\tau}p_1(n,T,\tau)\mathcal{N}_r[\tilde{\varepsilon}_r\lambda'^\tau_r + \tilde{\varepsilon}'_r\lambda^\tau_r]$$
$$+\sum_{r,\{\tau_1,\tau_2\}}p_1(n,T,\tau_1,\tau_2)\mathcal{N}_r[\lambda_r^{\tau_1}\lambda'^{\tau_2}_r + \lambda_r^{\tau_2}\lambda'^{\tau_1}_r]$$
$$+\sum_\tau p_2(n,T,\tau)\frac{2}{\mathcal{N}(\mathcal{N}+(-1)^\tau)}\sum{}^*[J]W^{J\tau}_{rstu}(2)W'^{J\tau}_{rstu}(2), \qquad (16)$$

where τ is 0 or 1, and the set $\{\tau_1,\tau_2\}$ is $\{0,0\}$, $\{0,1\}$ or $\{1,1\}$. The propagator functions are derived in [53,6] to be,

$$p_1(T) = \frac{n(\mathcal{N}+2)(\mathcal{N}-\frac{n}{2})-2\mathcal{N}T(T+1)}{\mathcal{N}(\mathcal{N}-1)(\mathcal{N}+1)} \qquad (17)$$

$$p_1(n,T,\tau) = \frac{4\mathcal{N}T(T+1)(1-n)(1-(-1)^\tau)+(\mathcal{N}+2)(\mathcal{N}-\frac{n}{2})[(2\tau+1)n(n+2(-1)^\tau)-4T(T+1)(-1)^\tau]}{4\mathcal{N}(\mathcal{N}-1)(\mathcal{N}+1)(\mathcal{N}+2(-1)^\tau)}$$

$$p_1(n,T,\tau_1,\tau_2) = \frac{1}{8(\mathcal{N}-1)(\mathcal{N}+1)(\mathcal{N}-2)(\mathcal{N}+2(-1)^{\tau_1})}\{4\mathcal{N}T(T+1)(n-1)\times$$
$$(\mathcal{N}-2n+4)(1-(-1)^{\tau_1}) + [(2\tau_1+1)n(n+2(-1)^{\tau_1}) - 4T(T+1)(-1)^{\tau_1}]\times$$
$$[(2\tau_2+1)(n+2(-1)^{\tau_2})(\mathcal{N}-\frac{n}{2})\tfrac{1}{2} + T(T+1)(-1)^{\tau_2}][\mathcal{N}-2(-1)^{\tau_2}]\}$$

$$p_2(n,T,\tau=0) = \frac{[n(n+2)-4T(T+1)][(\mathcal{N}-\frac{n}{2})(\mathcal{N}-\frac{n}{2}+1)-T(T+1)]}{8\mathcal{N}(\mathcal{N}-1)}$$

$$p_2(n,T,\tau=1) = \frac{1}{\mathcal{N}(\mathcal{N}+1)(\mathcal{N}-2)(\mathcal{N}-3)}\{\tfrac{1}{2}T^2(T+1)^2(3\mathcal{N}^2-7\mathcal{N}+6)$$
$$+\frac{3}{8}n(n-2)(\mathcal{N}-\frac{n}{2})(\mathcal{N}-\frac{n}{2}+1)(\mathcal{N}+1)(\mathcal{N}+2)$$
$$+\tfrac{1}{2}T(T+1)[(5\mathcal{N}-3)(\mathcal{N}+2)n(\frac{n}{2}-\mathcal{N})+\mathcal{N}(\mathcal{N}-1)(\mathcal{N}+1)(\mathcal{N}+6)]\}.$$

For the Sp(4) interaction, the average two-body interaction is expressed in terms of the model parameters in the scalar distribution as, $W_c = -\frac{3G_0}{\binom{\mathcal{N}}{2}} + \frac{3E_0}{2(\mathcal{N}-1)} - C$, and in the isospin-scalar case for a given isospin value as, $W_c^T = -\frac{G_0}{\binom{\mathcal{N}}{2}}\delta_{T1} + E_0[(-1)^T + \frac{1}{2}] - C$. The pure one-body part of the Sp(4) Hamiltonian is zero for a singe-j orbit (by definition) as well as for the $1f_{5/2}2p_{1/2}2p_{3/2}1g_{9/2}$ major shell (by assumption of constant interaction strengths). The pure two-body matrix elements, $W^{JT}_{rstu}(2)$, and hence the correlation coefficients involving $H_{\mathfrak{sp}(4)}$, are then independent of the C parameter in the scalar case and of the C and E_0 parameters in the isospin-scalar case.

References

[1] R. Machleidt, F. Sammarruca, and Y. Song, *Phys. Rev.* **C53**, R1483 (1996); R. Machleidt, *Phys. Rev.* **C63**, 024001 (2001).

[2] D. R. Entem and R. Machleidt, *Phys. Rev.* **C68**, 041001 (R) (2003).

[3] J. B. French and K. F. Ratcliff, *Phys. Rev.* **C3**, 94 (1971).

[4] F. S. Chang, J. B. French, and T. H. Thio, *Ann. Phys.* (N.Y.) **66**, 137 (1971).

[5] J. P. Draayer, *Nucl. Phys.* **A216**, 457 (1973).

[6] K. T. Hecht and J. P. Draayer, *Nucl. Phys.* **A223**, 285 (1974).

[7] T. R. Halemane, K. Kar, and J. P. Draayer, *Nucl. Phys.* **A311**, 301 (1978).

[8] V. K. B. Kota, *Phys. Rev.* **C20**, 347 (1979); Fortran Programs for Statistical Spectroscopy Calculations.

[9] G. Rosensteel, *Nucl. Phys.* **A341**, 397 (1980).

[10] V. K. B. Kota, S. P. Pandya, and V. Potbhare, *Nucl. Phys.* **A349**, 397 (1980).

[11] C. R. Countee, J. P. Draayer, T. R. Halemane, and K. Kar, *Nucl. Phys.* **A356**, 1 (1981).

[12] J. P. Draayer and G. Rosensteel, *Nucl. Phys.* **A386**, 189 (1982).

[13] S. Popescu, S. Stoica, J. P. Vary, and P. Navratil, to be published.

[14] M. Honma, T. Otsuka, B. A. Brown, and T. Mizusaki, *Phys. Rev.* **C69**, 034335 (2004).

[15] M. Hjorth-Jensen, T. T. S. Kuo, and E. Osnes, *Phys. Rep.* **261**, 125 (1995).

[16] K. D. Sviratcheva, A. I. Georgieva, and J. P. Draayer, Phys. Rev. **C69** 024313 (2004).

[17] K. D. Sviratcheva, A. I. Georgieva, and J. P. Draayer, Phys. Rev. **C70** 064302 (2004).

[18] K. D. Sviratcheva, J. P. Draayer, and J. P. Vary, *Phys. Rev.* **C73**, 034324 (2006).

[19] K. Langanke, *Nucl. Phys.* **A630**, 368c (1998).

[20] P. T. Hosmer et al., *Phys. Rev. Lett.* **94**, 112501 (2005).

[21] E. Caurier, G. Martinez-Pinedo, F. Nowacki, A. Poves, and A. P. Zuker, *Rev. Mod. Phys.* **77**, 427 (2005).

[22] B. A. Brown, *Prog. Part. Nucl. Phys.* **47**, 517 (2001).

[23] T. Otsuka, M. Honma, T. Mizusaki, N. Shimizu, and Y. Utsuno, *Prog. Part. Nucl. Phys.* **47**, 319 (2001).

[24] J. P. Draayer, J. B. French, V. Potbhare, and S. S. M. Wong, *Phys. Lett.* **55B**, 263, 349 (1975); J. P. Draayer, J. B. French, M. Prasad, V. Potbhare, and S. S. M. Wong, *Phys. Lett.* **57B**, 130 (1975); J. P. Draayer, J. B. French, and S. S. M. Wong, *Ann. of Phys.* **106**, 472, 503 (1977); B. D. Chang and J. P. Draayer, *Phys. Rev.* **C20**, 2387 (1979).

[25] V. Potbhare, *Nucl. Phys.* **A289**, 373 (1977).

[26] J. B. French, V. K. B. Kota, A. Pandey, and S. Tomsovic, Ann. Phys. (N.Y.) **181**, 235 (1988).

[27] V. K. B. Kota and D. Majumdar, Z. Phys. A **351**, 365 (1995); Z. Phys. A **351**, 377 (1995).

[28] S. Tomsovic, M. B. Johnson, A. Hayes, and J. D. Bowman, *Phys. Rev.* **C62**, 054607 (2000).

[29] J. M. G. Gomez, K. Kar, V. K. B. Kota, R. A. Molina, and J. Retamosa, *Phys. Lett.* **B 567**, 251 (2003).

[30] M. Horoi, M. Ghita, and V. Zelevinsky, *Phys. Rev.* **C69**, 041307(R) (2004); M. Horoi, J. Kaiser, and V. Zelevinsky, *Phys. Rev.* **C67**, 054309 (2003).

[31] W. Li et al., *Europhys. Lett.*, **64**, 750 (2003).

[32] N. D. Chavda, V. Potbhare, V. K. B. Kota, *Phys. Lett.*, **A 326**, 47 (2004).

[33] V. K. B. Kota, *Phys. Rev.* **C71**, 041304(R) (2005).

[34] D. Angom and V. K. B. Kota, *Phys. Rev.* **A71**, 042504 (2005).

[35] Y. M. Zhao, A. Arima, N. Yoshida, K. Ogawa, N. Yoshinaga, and V. K. B. Kota, *Phys. Rev.* **C72**, 064314 (2005).

[36] K. F. Ratcliff, *Phys. Rev.* **C3**, 117 (1971).

[37] J. B. French, in *Dynamic Structure of Nuclear States*, ed. D. J. Rowe *et al.* (Univ. of Toronto Press, Toronto, 1972), p.154.

[38] B. J. Dalton, W. J. Baldridge, and J. P. Vary, *Phys. Rev.* **C20**, 1908 (1979).

[39] J. B. French, *Nucl. Phys.* **A396**, 87c (1983).

[40] J. P. Draayer and G. Rosensteel *Phys. Lett.* **124B**, 281 (1983); J. P. Draayer and G. Rosensteel, *Phys. Lett.* **125B**, 237 (1983); G. Rosensteel and J. P. Draayer, *Nucl. Phys.* **A436**, 445 (1985).

[41] S. Sarkar, K. Kar, and V. K. B. Kota, *Phys. Rev.* **C36**, 2700 (1987).

[42] T. Otsuka et al., *Phys. Rev. Lett.* **87**, 082502 (2001).

[43] M. Dufour and A. P. Zuker, *Phys. Rev.* **C54**, 1641 (1996).

[44] J. C. Parikh, *Group Symmetries in Nuclear Structure* (Plenum, New York) (1978).

[45] J. Cohen, *Statistical Power Analysis for the Behavioral Sciences* (Lawrence Erlbaum Associates, Hillsdale, NJ) (1988); J. Cohen, P. Cohen, S. G. West, and L. S. Aiken, *Applied multiple regression/correlation analysis for the behavioral sciences*, 2nd ed. (Lawrence Erlbaum Associates, Hillsdale, NJ) (2003).

[46] K. T. Hecht, *Nucl. Phys.* **63**, 177 (1965); *Phys. Rev.* **139**, B794 (1965); *Nucl. Phys.* **A102**, 11 (1967); J. N. Ginocchio, *Nucl. Phys.* **74**, 321 (1965).

[47] J. Engel, K. Langanke, and P. Vogel, *Phys. Lett.* **B389**, 211 (1996).

[48] K. Kaneko, M. Hasegawa, and J. Y. Zhang, *Phys. Rev.* **C59**, 740 (1999).

[49] J. P. Elliott, *Proc. Roy. Soc.* (London) **A245**, 128 (1958); **A245**, 562 (1958); J. P. Elliott and M. Harvey, *Proc. Roy. Soc.* (London) **A272**, 557 (1963).

[50] B.D. Chang, *Nucl. Phys.* **A304**, 127 (1978).

[51] J. B. French, *Phys. Lett.* **26B**, 75 (1967).

[52] B. D. Chang, J. P. Draayer, and S. S. M. Wong, *Comput. Phys. Commun.* **28**, 41 (1982).

[53] J. B. French, in *Isospin in Nuclear Physics*, ed. D. H. Wilkinson (North Holland,Amsterdam, 1969), p.259

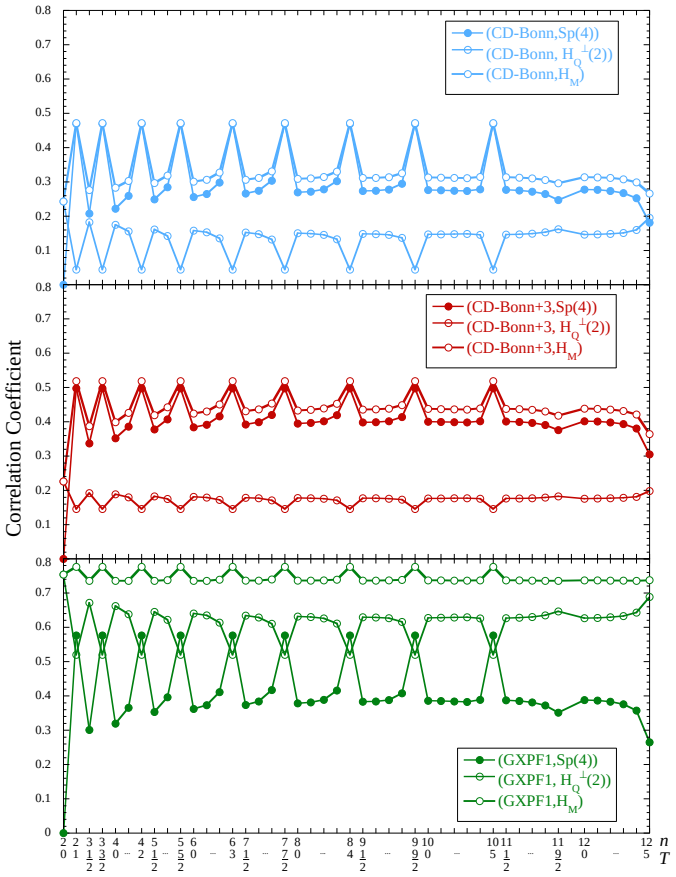

Fig. 1. Correlation coefficients of the pure two-body "CD-Bonn" (blue), CD-Bonn+3terms (red) and GXPF1 (green) interactions with $H_{\mathfrak{sp}(4)}$ (filled symbols), $H_{\overline{Q}}^{\perp}(2)$ (transparent symbols) and H_M (empty symbols) in the upper *fp* shell for the isospin-scalar distribution. For each valence particle number, n, the isospin T varies as $\frac{n}{2}, \frac{n}{2}-1, \ldots, 0(\frac{1}{2})$. The figures are symmetric with respect to the sign of $n-2\Omega$ ($\Omega=6$).

Table 2
Scalar distribution correlation coefficients for many-nucleon systems of the $H_0(2)$ pure two-body part of the "CD-Bonn", CD-Bonn+3terms and GXPF1 interactions with H_M (Eq. 3), $H_{\mathfrak{sp}(4)}$ (Eq. 4), $H_{\overline{Q}}^{\perp}(2)$, and with the pure two-body full quadrupole-quadrupole interaction, $H_Q(2)$. The $R_{\mathrm{Sp}(4)} = (\zeta_{H_M,H_{\mathfrak{sp}(4)}})^2$ quantity gives the part, in %, of H_M that is Sp(4) symmetric.

	"CD-Bonn"	CD-Bonn+3terms	GXPF1
$\zeta_{H_0(2),H_M}$	0.57	0.54	0.83
$\zeta_{H_0(2),H_{\mathfrak{sp}(4)}}$	0.55	0.50	0.65
$\zeta_{H_0(2),H_{\overline{Q}}^{\perp}(2)}$	0.14	0.20	0.51
$\zeta_{H_0(2),H_Q(2)}$	0.28	0.33	0.67
$R_{\mathrm{Sp}(4)}$	93.1%	85.7%	61.3%

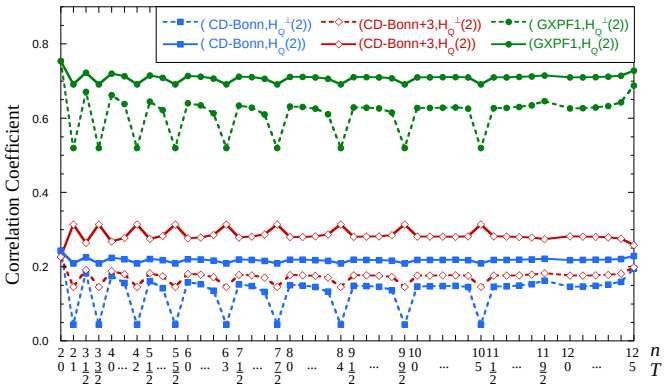

Fig. 2. Comparison between the orthogonal $H_Q^{\perp}(2)$ and the full two-body $H_Q(2)$ quadrupole-quadrupole interactions in their correlation to the pure two-body part of the fp-shell interactions, "CD-Bonn" (blue squares), CD-Bonn+3terms (red diamonds) and GXPF1 (green circles), in the isospin-scalar distribution. For each valence particle number, n, the isospin T varies as $\frac{n}{2}, \frac{n}{2}-1, \ldots, 0(\frac{1}{2})$. The figure is symmetric with respect to the sign of $n-2\Omega$ ($\Omega=6$).

Table 3
Correlation coefficients for many-nucleon systems of the "CD-Bonn", CD-Bonn+3terms and GXPF1 interactions, H_0, with H_M(Eq. 3), $H_{\mathfrak{sp}(4)}$(Eq. 4), and the full quadrupole-quadrupole interaction, H_Q. The $R_{\mathrm{Sp}(4)} = (\zeta_{H_M,H_{\mathfrak{sp}(4)}})^2$ quantity gives the part, in %, of H_M that is Sp(4) symmetric.

		Scalar Distribution		
		$1f_{7/2}$	$1f_{5/2}$	$2p_{1/2}2p_{3/2}{}^a$
"CD-Bonn"	ζ_{H_0,H_M}	0.81	0.76	0.61
	$\zeta_{H_0,H_{\mathfrak{sp}(4)}}$	0.66	0.70	0.58
	ζ_{H_0,H_Q}	0.69	0.64	0.17
	$R_{\mathrm{Sp}(4)}$	65.9%	83.7%	91.7%
CD-Bonn+3terms	ζ_{H_0,H_M}	0.87	0.86	0.52
	$\zeta_{H_0,H_{\mathfrak{sp}(4)}}$	0.64	0.67	0.51
	ζ_{H_0,H_Q}	0.80	0.82	0.22
	$R_{\mathrm{Sp}(4)}$	53.4%	60.6%	98.3%
GXPF1	ζ_{H_0,H_M}	0.93	0.84	0.90
	$\zeta_{H_0,H_{\mathfrak{sp}(4)}}$	0.76	0.77	0.70
	ζ_{H_0,H_Q}	0.78	0.69	0.85
	$R_{\mathrm{Sp}(4)}$	67.9%	84.7%	61.7%

[a] pure two-body part of the interactions

Table 4
Correlation coefficients for a two-nucleon system of the "CD-Bonn", CD-Bonn+3terms and GXPF1 interactions, H_0, with H_M(Eq. 3) and $H_{\mathfrak{sp}(4)}$(Eq. 4). $R_{\mathrm{Sp}(4)} = (\zeta_{H_M,H_{\mathfrak{sp}(4)}})^2$ gives the part, in %, of H_M that is Sp(4) symmetric.

Isospin-scalar Distribution, $T = 1$				
		$1f_{7/2}$	$1f_{5/2}$	$2p_{1/2}2p_{3/2}{}^a$
"CD-Bonn"	$\zeta^{T=1}_{H_0,H_M}$	0.95	1.00	0.59
	$\zeta^{T=1}_{H_0,H_{\mathfrak{sp}(4)}}$	0.61	0.57	0.54
	$R_{\mathrm{Sp}(4)}$	41.5%	32.3%	84.2%
CD-Bonn	$\zeta^{T=1}_{H_0,H_M}$	0.98	1.00	0.61
+3terms	$\zeta^{T=1}_{H_0,H_{\mathfrak{sp}(4)}}$	0.85	0.93	0.59
	$R_{\mathrm{Sp}(4)}$	73.9%	86.9%	92.1%
GXPF1	$\zeta^{T=1}_{H_0,H_M}$	0.96	1.00	0.94
	$\zeta^{T=1}_{H_0,H_{\mathfrak{sp}(4)}}$	0.71	0.86	0.69
	$R_{\mathrm{Sp}(4)}$	54.5%	74.0%	53.5%

[a] pure two-body part of the interactions

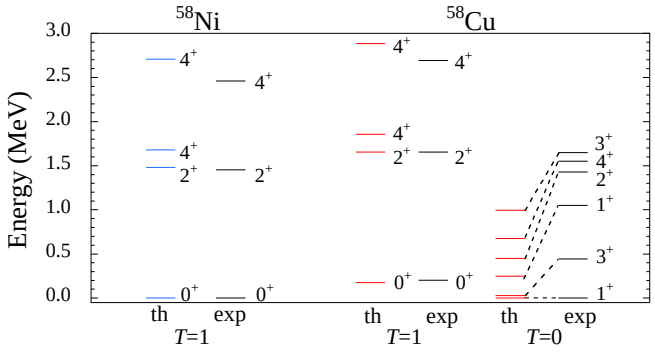

Fig. 3. Theoretical ('th') low-lying energy spectra for ^{58}Ni (left, blue) and ^{58}Cu (right, red) compared to experiment ('exp', black). The theoretical calculations are performed in the $1f_{5/2}2p_{1/2}2p_{3/2}1g_{9/2}$ major shell with the H_M model interaction (Eq. 3 with $\chi = 0.027$) and with single-particle energies derived from ^{57}Ni experimental energy levels.